Journal of Cellular Biochemistry 103:1925–1937 (2008)

Astaxanthin Protects Mesangial Cells From Hyperglycemia-Induced Oxidative Signaling

Emiko Manabe,[1] Osamu Handa,[2] Yuji Naito,[3]* Katsura Mizushima,[4] Satomi Akagiri,[4] Satoko Adachi,[4] Tomohisa Takagi,[2] Satoshi Kokura,[2] Takashi Maoka,[5] and Toshikazu Yoshikawa[4]

[1]School of Nursing, Kyoto Prefectural University of Medicine, Kyoto, 602-8566 Japan
[2]Department of Biomedical Safety Science, Kyoto Prefectural University of Medicine, Kyoto, 602-8566 Japan
[3]Department of Medical Proteomics, Kyoto Prefectural University of Medicine, Kyoto, 602-8566 Japan
[4]Department of Inflammation and Immunology, Kyoto Prefectural University of Medicine, Kyoto, 602-8566 Japan
[5]Research Institute for Production Development, Kyoto, 606-0805 Japan

Abstract Astaxanthin (ASX) is a carotenoid that has potent protective effects on diabetic nephropathy in mice model of type 2 diabetes. In this study, we investigated the protective mechanism of ASX on the progression of diabetic nephropathy using an in vitro model of hyperglycemia, focusing on mesangial cells. Normal human mesangial cells (NHMCs) were cultured in the medium containing normal (5 mM) or high (25 mM) concentrations of D-glucose. Reactive oxygen species (ROS) production, the activation of nuclear transcription factors such as nuclear factor kappa B (NFκB) and activator protein-1 (AP-1), and the expression/production of transforming growth factor-beta 1 (TGFβ_1) and monocyte chemoattractant protein-1 (MCP-1) were evaluated in the presence or absence of ASX. High glucose (HG) exposure induced significant ROS production in mitochondria of NHMCs, which resulted in the activation of transcription factors, and subsequent expression/production of cytokines that plays an important role in the mesangial expansion, an important event in the pathogenesis of diabetic nephropathy. ASX significantly suppressed HG-induced ROS production, the activation of transcription factors, and cytokine expression/production by NHMCs. In addition, ASX accumulated in the mitochondria of NHMCs and reduced the production of ROS-modified proteins in mitochondria. ASX may prevent the progression of diabetic nephropathy mainly through ROS scavenging effect in mitochondria of mesangial cells and thus is expected to be very useful for the prevention of diabetic nephropathy. J. Cell. Biochem. 103: 1925–1937, 2008.

Key words: mesangial cell; hyperglycemia; mitochondria; lipid peroxidation; nuclear transcription factors; diabetic nephropathy

The world's diabetic population stood at roughly 171 million in 2000, and the number is predicted to increase to 366 million by 2030 [Wild et al., 2004]. The most common complications associated with diabetes mellitus consist of retinopathy, neuropathy, and nephropathy. Importantly, growing number of diabetic nephropathy patients who require chronic dialysis treatment has been reported in many areas in the world [Lok et al., 2004; Nakai et al., 2006].

Abbreviations used: 4HNE, 4-hydroxy-2-nonenal; 8-OHdG, 8-hydroxy-deoxyguanosine; 8-oxodG, 8-oxo-7,8-dihydro-2′-deoxyguanosine; AP-1, activator protein-1; ASX, astaxanthin; CCCP, carbonyl cyanide m-chlorophenylhydrazone; COX, cytochrome C oxidase; COX-2, cyclooxygenase-2; DTT, dithiothreitol; EMSA, Electro-Mobility Gel-Shift assay; FITC, fluorescein isothiocyanate; HG, high glucose; HPLC, high performance liquid chromatography; LDH, lactate dehydrogenase; MCP-1, monocyte chemoattractant protein-1; MnSOD, manganese superoxide dismutase; NG, normal glucose; NFκB, nuclear factor kappa B; NHMCs, normal human mesangial cells; ROS, reactive oxygen species; TTFA, thenoyltrifluoroacetone; TGFβ_1, transforming growth factor-beta 1; UCP-1, uncoupling protein-1.

Emiko Manabe and Osamu Handa contributed equally to this work.

*Correspondence to: Yuji Naito, Department of Medical Proteomics, Kyoto Prefectural University of Medicine, Kajiicho, Kawaramachidori Hirokouji Agaru, Kamigyou-ku, Kyoto, 602-8566 Japan. E-mail: ynaito@koto.kpu-m.ac.jp

Received 29 May 2007; Accepted 23 August 2007
DOI 10.1002/jcb.21583

Since the progress of diabetic nephropathy is mostly irreversible and has an extremely poor prognosis, it is important to prevent the onset and progression of the nephropathy in the early stage of diabetes mellitus.

Production of reactive oxygen species (ROS) in mitochondria has been reported to have an impact not only on the development of diabetes but also on its complications [Baynes and Thorpe, 1999; Kaneto et al., 2007]. For example, ROS production is increased in diabetic patients, especially in those who are with poor glycemic control. In addition, randomized clinical trial revealed that the intensive glycemic control reduced or normalized mitochondrial ROS production and consequently delayed the onset and progression of early stage of diabetic microvascular and macrovascular complication [Nishikawa et al., 2007]. Increased levels of oxidative stress markers such as 8-oxo-7,8-dihydro-2′-deoxyguanosine (8-oxodG, a maker of DNA oxidation) in urine or leukocytes were reported to correlate with the severity of diabetic nephropathy and retinopathy [Hinokio et al., 1999], and the increased levels of 8-hydroxy-deoxyguanosine (8-OHdG, a maker of DNA oxidation) was also demonstrated in the muscle of diabetic patients with nephropathy [Suzuki et al., 1999]. Therefore, we supposed that we could prevent the onset of diabetic nephropathy by suppressing oxidative stress. One of candidate suppressors of oxidative stress is a dietary antioxidant supplementation that is easy to intake, less toxic, and cheap.

Astaxanthin (ASX), which is found as a common pigment in algae, fish, and birds is a carotenoid that has potent pharmacological effects, such as antioxidative- [Fukuzawa et al., 1998; Kobayashi, 2000; Naguib, 2000], immunomodulating- [Jyonouchi et al., 1994, 1995; Kurihara et al., 2002], anticancer- [Chew et al., 1999], and anti-inflammatory- [Bennedsen et al., 1999; Ohgami et al., 2003] actions. The antioxidant activity of ASX is greater than that of β-carotene or α-tocopherol, and one of the effects of ASX is to scavenge ROS, such as singlet oxygen, superoxide radicals, and lipid peroxyl radicals [Fukuzawa et al., 1998; Naguib, 2000].

The predominant structural changes seen in diabetic nephropathy are extracellular matrix accumulation of proteins such as collagen, laminin, and fibronection, which lead to mesangial expansion and glomerular basement membrane thickening [Coughlan et al., 2007] that is induced by cytokines produced by mesangial cells. We have previously reported that oral treatment with ASX alleviated albuminuria, but also glomerular histological changes in db/db mice, a rodent model of type 2 diabetes, with little effects on blood glucose levels, the effect being accompanied by decreased urinary excretion of 8-OHdG. Especially, we found that oral treatment of diabetic mice with ASX reduced hyperglycemia-induced 8-OHdG expression in mesangial lesions as assessed by immunohistochemical staining and reduced mesangial expansion. We therefore concluded that hyperglycemia-induced oxidative stress might be a crucial mechanism of diabetic renal damage and the suppression of oxidative stress in mesangial lesions by ASX might be a novel approach for the prevention of diabetic nephropathy [Uchiyama et al., 2002; Naito et al., 2004]. However, it is unclear as to how ASX ameliorates the renal damage induced by high glucose (HG) levels. In the present study, we investigated the protective effects of ASX in vitro using normal human mesangial cells mainly focused on the molecular mechanisms of cytokine production that is important for mesangial expansion.

MATERIALS AND METHODS

Reagents

D-glucose was from Otsuka Pharmaceutical Co. Ltd. (Tokyo, Japan); L-glucose, from MP Biomedicals (Eschwege, Germany); MsBM, from Cambrex (Long Beach, CA); fetal bovine serum (FBS), from EQUITECH-BIO. Inc. (Kerrville, TX) and phosphate-buffered saline (PBS), from Nissui Pharmaceutical Co. Ltd. (Tokyo, Japan); bovine serum albumin, from Sigma Chemical (St. Louis, MO); trypsin EDTA, from Gibco BRL (Carlsbad, CA); dimethyl sulfoxide (DMSO), acetone, and methanol were from Wako Pure Chemical Industries, Ltd. (Osaka, Japan).

A rabbit polyclonal antibody directed against nuclear factor kappa B (NFκB) subunit, RelA (p65), and goat-anti-rabbit IgG were from Santa Cruz Biotechnology Inc. (Santa Cruz, CA). A rabbit polyclonal antibody directed against 4-hydroxy-2-nonenal (4HNE) was kindly provided by Professor Koji Uchida (Nagoya University, Nagoya, Japan).

ASX was from Sigma Chemical (St. Louis, MO), dissolved in DMSO and diluted in PBS with 5% FBS. In a clinical study [Coral-Hinostroza et al., 2004], it has been shown that 10 mg of ASX administered to three healthy adults resulted in their plasma concentration of ASX ranging 0.08–0.28 mg/L (1.3×10^{-7}–5×10^{-7} M) [Coral-Hinostroza et al., 2004]. Therefore, ASX at the final concentration of 10^{-7}–10^{-4} M in 0.05% DMSO in PBS with 5% FBS were used in this study. As a control condition, 0.05% DMSO in PBS with 5% FBS were used.

Cell Line

Normal human mesangial cells, (NHMCs; Cambrex, Long Beach, CA) at passage 5–10 were used. The cells were maintained in MsBM, supplemented with 5% FBS, 50 mg/ml gentamicin and 50 mg/ml amphotericin-B. The cell culture medium was changed every 3 days. The cells were incubated at 37°C in humidified atmosphere with 5% CO_2. When NHMCs were fully confluent, these cells were tripsinized and seeded into each adequate apparatus described below.

Cell Viability Assay

Cell viability of NHMCs was assessed using MTT-based assay (WST-1, Cell Counting Kit, Dojin Laboratory, Kumamoto, Japan) and lactate dehydrogenase (LDH) release.

Briefly, NHMCs were cultured in 96-well plates, and were incubated in the medium containing 5 mM (normal glucose: NG) or 25 mM HG of D-glucose and/or ASX (10^{-4} or 10^{-5} M) for 48 h. Subsequently, the cells were washed and incubated with 5 mM of WST-1 solution for 2 h at 37°C, and the optical density of each well was read at wave length of 450 nm by MPR-A4i microplate reader (Tosoh, Tokyo, Japan).

At the same time, LDH release in the cell supernatant, the marker of cell death was measured using a MTX-LDH kit (Kyokuto-seiyaku Co. Ltd., Tokyo, Japan). Briefly, a 50 ml of cell culture supernatant was mixed with 37 ml of nitrotetrazolum blue, and LDH was quantified by the rate of change in absorbance at wavelength of 560 nm for 30 min at 37°C by MPR-A4i.

Production of Reactive Oxygen Species (ROS)

Confluent NHMCs cultured on labtek chamber slide were pre-incubated with or without ASX (10^{-6} M) for 24 h, washed with PBS, and were further incubated with NG or HG for 30 min. Subsequently the cells were washed with PBS and stained with 1 mM of mitochondria-selective fluorescent probe, MitoTracker Green FM (Molecular Probes; Eugene, OR) and 0.1 mM of redox-sensitive fluorescent probe, RedoxSensor Red CC-1 (Molecular Probes). ROS production in mitochondria was observed under a confocal laser scanning microscopy (FV1000; Olympus, Tokyo, Japan) using sequential activation of each fluorescence. Photographic images were taken from four random fields.

Immunocytochemical Staining for NFκB

Confluent NHMCs cultured on labtek chamber slide glass were pre-incubated with or without ASX (10^{-6} M) for 24 h, washed with PBS, and were further incubated with NG or HG for 60 min. Immunocytochemical staining method was the same as described before [Handa et al., 2004]. Briefly, cells were fixed with a mixture of acetone and methanol, incubated with a rabbit polyclonal antibody directed against NFκB subunit, RelA (p65) for 2 h at room temperature, and then incubated with fluorescein isothiocyanate (FITC)-conjugated goat-anti-rabbit IgG (Santa Cruz Biotechnology Inc.) for 2 h at room temperature. NFκB nuclear translocation images were taken from four random fields using FV1000.

Electro-Mobility Gel-Shift Assay (EMSA) for Nuclear Transcription Factors

Experimental settings were the same as described in NFκB translocation assay except for NHMCs being cultured in 6-cm cell culture dishes. Nuclear protein fractions were extracted and the method for EMSA was same as described before [Cepinskas et al., 2003; Handa et al., 2006b]. Briefly, 10 mg of total extracted nuclear proteins was incubated with 1.0 pmol double-stranded [^{32}P] ATP end-labeled oligonucleotides containing consensus binding sequences for NFκB (sense strand: 5′-AGTT-GAGGGGACTTTCCCAGGC-3′ and antisense strand: 3′-TCAACTCCCCTGAAAGGGTCCG-5′) or for activator protein-1 (AP-1), (sense strand: 5′-d(CGCTTGATGAGTCAGCCGGAA)-3′ and antisense strand: 3′-d(GCGAACTACTCAGTCGG-CCTT)-5′) in binding buffer (10 mM Hepes, pH 7.9, 80 mM NaCl, 3 mM $MgCl_2$, 0.1 mM EDTA, 1 mM DTT, 1 mM PMSF, and 10% glycerol). After the electrophoresis, gels were

dried and radioactive bands were visualized on X-ray films. Band intensity of NFκB and AP-1 was densidometrically quantified using Image J program (National Institutes of Health, Bethesda, MD).

ELISA for TGFβ$_1$ and MCP-1 Production

Transforming growth factor beta 1 (TGFβ$_1$) production in cell culture supernatant was assessed using an ELISA kit (R&D Systems Inc., Minneapolis) according to the manufacturer's instructions. Confluent NHMCs in 96-well plates were pre-incubated with or without ASX (10^{-6} M) for 24 h, washed with PBS, and were further incubated with NG or HG for 24 or 48 h. After centrifugation of 96-well plates, cell culture supernatant (200 μl) was removed from each well and treated with 40 μl of 1 N HCl for 10 min at room temperature to activate latent TGFβ$_1$. After neutralization (to pH 7.2–7.6) of acidified samples by 40 μl of 1.2 N NaOH/0.5 HEPES solution, 200 μl of standard or activated samples were placed into 96-well plates coated with recombinant human TGFβ$_1$ receptor type 2 and incubated for 3 h at room temperature. Then the plate was washed with wash buffer, added 200 μl of a horseradish peroxidase-conjugated polyclonal anti-TGFβ$_1$ antibody, and incubated at room temperature for further 90 min. A volume of 200 μl of substrate solution (1:1 mixture of H_2O_2 and the chromogen tetramethylbenzidine solution) was added to each well. The amount of activated TGFβ$_1$ was determined colorimetrically at 450 nm wavelength by MPR-A4i using tetramethylbenzidine as a substrate.

Monocyte chemoattractant protein-1 (MCP-1) production was also measured by ELISA kit (Biosource International, Camarillo, CA). For MCP-1, experimental settings were the same as those in TGFβ$_1$ and 50 μl cell supernatants were added to MCP-1 antibody-coated 96-well plates. After the addition of biotinylated anti-MCP-1 and streptavidin-peroxidase, tetramethylbenzidine was used as a stabilized chromogen. The absorbance of each well was read at 450 nm by MPR-A4i.

Real Time Polymerase Chain Reaction (Real Time PCR)

Confluent NHMCs in 6-cm cell culture dishes were pre-incubated with or without ASX (10^{-6}, 10^{-7} M) for 24 h, washed with PBS, and were further incubated with NG or HG for 60 min. Total RNA was isolated with acid guanidinium phenol chloroform method using ISOGEN reagent (Nippon Gene, Toyama, Japan). The RNA concentration was determined spectrophotometrically at 260/280 nm. The RNA was used for real time PCR amplification. An aliquot (1 ng) of extracted RNA was reverse-transcribed into first-strand complementary DNA (cDNA) at 42°C for 30 min, using 100 U/ml reverse-transcriptase (Takara Biochemicals, Shiga, Japan) and 0.1 mM of oligo (dT)-adapter primer (Takara) in a 20 ml reaction mixture. RT-PCR was carried out with a 7300 Real Time PCR system (Applied Biosystems, Foster City, CA) using the DNA-binding dye SYBER Green 1 for the detection of PCR products. The reaction mixture (RT-PCR kit, Code RRo43A, Takara) contained 12.5 ml Premix Ex Taq, Rox reference dye, and 2 μl of cDNA to give final reaction volume of 25 ml. Primers were as follows: for TGFβ$_1$, sense: 5′-CCGCGGGACTATCCACCT-3′ and antisense: 5′-ATGGCCTCGATGCGCTT-3′, for MCP-1, sense: 5′-CGCCTCCAGCATGA-AAGTCT-3′ and antisense: 5′-GGAATGAAGG-TGGCTGCTATG-3′, and for cyclooxygenase-2 (COX-2), sense: 5′-GAAGCACTCTATGGTGA-CATCGAT-3′ and antisense: 5′-GCATCTGGC-CGAGGCTTT-3′. The PCR settings were as follows: initial denaturation of 15 s at 95°C was followed by 40 cycle of amplification for 15 s at 95°C and 31 s at 60°C. The PCR products were quantified using standard DNA for each purified by PCR products of reverse-transcribed RNA. The relative expression was then calculated as the density of the product of the respective target gene divided by that for GAPDH from the same cDNA.

Fractioning for Mitochondrial/Cytosolic Proteins

NHMCs were fractionated into cytosol and mitochondria by using a mitochondrial/cytosol fractionation kit (BioVision Research Products; CA) according to the manufacturer's instructions with some modifications. Briefly, cells were incubated with Cytsol Extraction Buffer without dithiothreitol (DTT) on ice for 10 min were homogenized with the grinder and centrifuged at 700*g* for 10 min at 4°C. The pellet was discarded and the supernatant was further centrifuged at 1,000*g* for 30 min at 4°C. The supernatant (cytosolic fraction) and pellet (mitochondrial fraction) were collected separately, and mitochondrial fraction was re-suspended with Mitochondrial Extraction

Buffer (without DTT). The purity of mitochondrial fraction was determined by using mouse monoclonal antibody against cytochrome C oxidase complex IV subunit (COX) of mitochondrial electron transport chain (Molecular Probes), a well-known mitochondrial protein marker.

Western Blotting for Mitochondrial/Cytosolic Proteins

Five dishes (10-cm cell culture dishes) of confluent NHMCs in each group were pre-incubated with or without ASX (10^{-6} M) for 24 h, washed with PBS, and were further incubated with NG or HG for 24 h. Subsequently, the cells were fractionated into mitochondrial/cytosolic fraction by the above described method. These fractions were incubated with 4× sample buffer without mercaptoethanol (Invitrogen, Carlsbad, CA) and denatured at 70°C for 10 min. Twenty micrograms of protein was electrophoresed on 4–20% gradient SDS–polyacrylamide gel and transferred to polyvinylidene fluoride membranes (Amersham Bioscience, Buckinghamshire, England) using an semi-dry electrophoretic transfer unit (Nippon Eido, Tokyo, Japan) at a constant current of 180 mA for 1 h in a transfer buffer containing 25 mM Tris, 192 mM glycine, and 10% methanol. Transferred membranes were incubated for 60 min in a blocking solution (5% skim milk). Then the membranes were treated with a rabbit anti-human 4HNE polyclonal antibody in PBS with 0.1% Tween-20 for overnight. ECL anti-rabbit IgG_1 horseradish peroxidase-linked antibody (Amersham Bioscience) was used as a secondary antibody and the ECL Western blotting detection reagent (Amersham) was used to optimize the primary antibody, and bands were visualized on hyperfilm ECL (Amersham). Band intensity of 4HNE in mitochondrial fraction was densidometrically quantified with that of COX as a control using Image J program (National Institutes of Health, Bethesda, MD).

Quantitative Analysis of ASX Concentration in Mitochondria and Cytoplasm

ASX content in mitochondrial and cytosolic fractionation was quantified by high performance liquid chromatography (HPLC). Five dishes (10-cm cell culture dishes) of confluent NHMCs in each group were pre-incubated with or without ASX (10^{-5} or 10^{-6} M) for 24 h, washed with PBS, and NHMCs were fractionated into cytosol and mitochondria as described above. The fractionation was evaporated to dryness. The residue was dissolved in 200 ml of acetone and filtered through a 0.45-mm polytetrafluoroethylene membrane filter; then 20 ml of solution was subjected to HPLC on a Shimadzu SPD-6AV spectrophotometer (Shimadzu, Kyoto, Japan) set at 460 nm. The column used was a Wakosil $5C_{18}$ (ODS) column (250 nm length × 4.6 mm internal diameter) with a mobile phase of methyl alcohol. A low rate was used (1.0 ml/min). ASX was quantified relative to calibration with a standard sample (F. Hoffman-La Roche Ltd., CA). Obtained quantity of ASX in total mitochondria in samples was adjusted by added total ASX quantity and expressed as % of added total ASX.

Statistical Analysis

The results are presented as the mean ± SEM. Two-way ANOVA was used to assess the differences between multiple groups. If the F statistic was significant, the mean values obtained from each group were then compared by Bonferroni's method. $P < 0.05$ was used as the criterion for statistically significant difference. Statistical analysis was performed using the SPSS12.0-J program (SPSS Japan, Inc., Tokyo, Japan).

RESULTS

HG and ASX Did Not Affect Cell Viability of NHMCs

As shown in Figure 1A, incubation of NHNCs with HG in the absence or presence of ASX did not affect NHMCs viability for 48 h as assessed by WST-1. ASX itself did not affect NHMCs viability within 48 h.

These findings were further confirmed by measuring LDH release into the cell culture medium. Same as the result obtained in WST-1 assay, HG or/and ASX did not affect LDH release by NHMCs (Fig. 1B). In addition, high concentration of L-glucose (25 mM, osmotic control) did not affect cellular viability of NHMCs as assessed by WST-1 assay and LDH release (data not shown).

ASX Reduced HG-Induced Mitochondria-Dependent ROS Production in NHMCs

As shown in Figure 2, mitochondria were equally stained with MitoTracker Green FM in

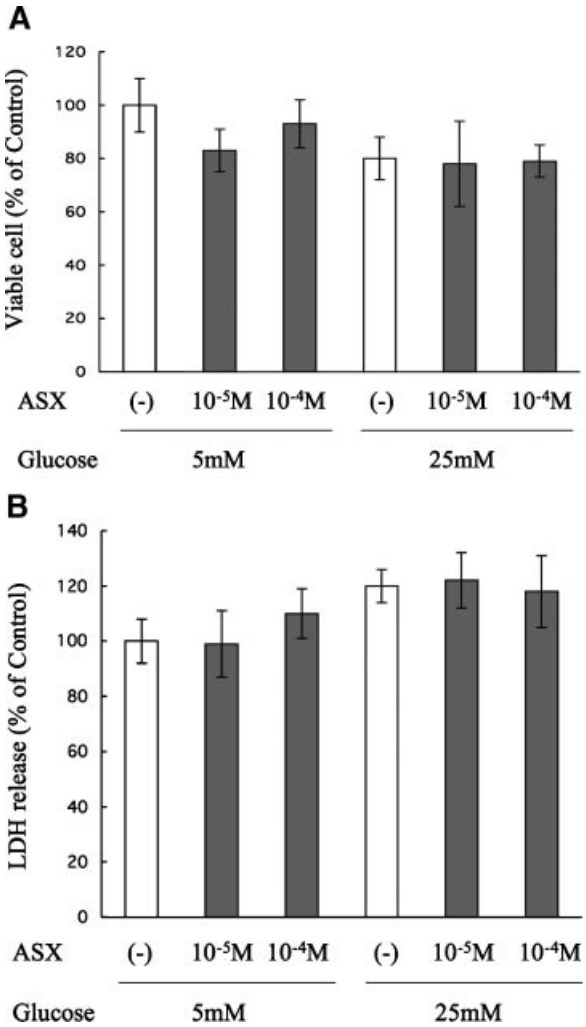

Fig. 1. HG and ASX did not affect cellular viability. Cell viability assessed by WST-1 assay (**A**) and LDH release (**B**) was presented. The results are given as percentage variation of O.D. versus NG (5 mM of D-glucose alone) group. Data are presented as mean ± SEM of nine independent experiments performed in triplicate samples.

each group. In contrast, fluorescent intensity of RedoxSensor Red CC-1 was increased in HG-exposed NHMCs, indicating the increased production of ROS (H_2O_2, $HOO^{\cdot}$, or $O_2^{\cdot -}$) in HG-exposed NHMCs (Fig. 2B). Merged images clearly indicated that mitochondria are the major source of ROS production in HG-exposed NHMC. Pre-treatment of NHMCs with ASX reduced HG-induced ROS production in mitochondria of NHMCs (Fig. 2D). ASX itself did not affect ROS production in NHMCs (Fig. 2C).

ASX Suppressed HG-Induced Activation of NFκB

NFκB translocation from the cytoplasm to the nuclei is a crucial step for NFκB activation. The images obtained by a laser scanning confocal microscopy indicated that p65 subunit of NFκB was localized exclusively to the cell cytoplasm in NHMCs cultured in NG (Fig. 3A, upper left). However, incubation of NHMCs with HG for 1 h resulted in apparent translocation of p65 to the cell nuclei (Fig. 3A, upper right). In addition, pre-incubation of NHMCs with ASX for 24 h prevented this HG-induced nuclear translocation of p65 in NHMCs (Fig. 3A, lower right). ASX itself did not affect p65 localization (Fig. 3A, lower left).

To provide more direct evidence, DNA-binding activity of NFκB was assessed by EMSA. Analysis of nuclear extracts from HG-incubated NHMCs demonstrated that the binding activity of NFκB was significantly higher than that in NG-incubated cells. Moreover, pre-incubation of NHMCs with ASX for 24 h inhibited the HG-induced increase in NFκB-binding activity (Fig. 3B). ASX itself did not affect NFκB activation in NHMCs.

ASX Inhibited the Expression/Production of MCP-1 and Expression of COX-2

As shown in Figure 4A and B, incubation of NHMCs with HG for 48 h induced a significant increase of the expression/production of MCP-1. In addition, pre-incubation of NHMCs with ASX significantly reduced HG-induced MCP-1 expression/production compared to that in control group. ASX itself did not affect MCP-1 expression/production by NHMCs. Similarly, HG-induced expression of COX-2 were significantly reduced by ASX pretreatment (Fig. 4C).

ASX Suppressed HG-Induced Activation of AP-1

DNA-binding activity of AP-1 was also assessed by EMSA. Similar to the results obtained in NFκB assay, HG induced significant activation of AP-1 in NHMCs. Pre-incubation of NHMCs with ASX for 24 h also inhibited the HG-induced increase in AP-1-binding activity (Fig. 5). ASX itself did not affect AP-1 activation in NHMCs.

ASX Inhibited the Expression/Production of TGFβ_1

As shown in Figure 6A and B, incubation of NHMCs with HG for 48 h induced a significant increase of the expression/production of TGFβ_1. In addition, pre-incubation of NHMCs with ASX significantly reduced HG-induced TGFβ_1

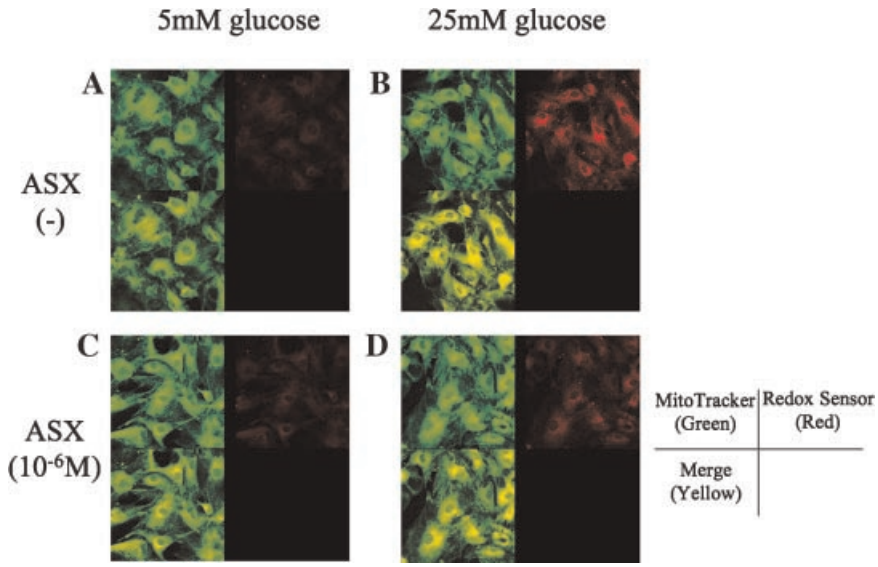

Fig. 2. ASX reduced HG-induced mitochondria-dependent ROS production in NHMCs. The laser scanning confocal microscopic image of NHMCs treated with (**A**) NG, (**B**) HG, (**C**) NG + ASX, and (**D**) HG + ASX were presented. In each panel, the image of mitochondria (MitoTracker: green fluorescence) and ROS production (RedoxSensor: red fluorescence) were presented in the **upper panel**, and merged (yellow fluorescence) images were presented in the **lower panel**. A representative image out of three independent experiments performed in triplicate samples were presented. [Color figure can be viewed in the online issue, which is available at www.interscience.wiley.com.]

expression/production compared to that in control group. ASX itself did not affect TGFβ_1 expression/production by NHMCs.

ASX Was Accumulated in Mitochondria of NHMCs

ASX (10^{-5}, 10^{-6} M) added to NHMCs was clearly accumulated in mitochondria but not in cytosol of NHMCs as assessed by HPLC (Table I).

ASX Suppressed the Production of Lipid Peroxidation of Mitochondrial Proteins

Since mitochondria is one of the major site for ROS generation, we analyzed the production of 4-hydroxy-2,3-nonenal (4HNE) protein adducts as a maker of oxidative lipid oxidation [Uchida, 2005], since 4HNE is an aldehydic molecule generated endogenously during the process of lipid peroxidation. We found that HG induced at least three 4HNE protein adducts production (bands) in mitochondrial fraction that were significantly reduced by pretreatment of NHMCs with ASX (Fig. 7A,B). 4HNE protein adducts production were also found in cytosolic fraction in HG-treated NHMCs in lesser extent than that in mitochondrial fraction that was suppressed by ASX pre-treatment.

DISCUSSION

Oxidative stress caused by chronic high blood glucose levels has been reported to involve in the onset and progression of diabetes mellitus [Ha and Lee, 2001; Lee et al., 2003]. The increases in oxidative stress in the kidney of diabetic patients originates from renal vascular endothelial cells [Inoguchi et al., 2000; Nishikawa et al., 2000; Lee et al., 2003] as well as from mesangial cells [Catherwood et al., 2002; Kang et al., 2003]. Mesangial cells are cells that not only surround vascular endothelium in the glomerulus, and produce the extra cellular matrix to support surrounding cells [Ziyadeh, 1993] but also produce cytokines that interact with vascular endothelial cells or inflammatory cells. In addition, the overproduction of mesangial matrix is a most important event in the pathogenesis of diabetic nephropathy. Recently, we found that ASX prevented the onset of diabetic nephropathy using an animal model of type 2 diabetes [Naito et al., 2004]. Therefore, in the present study, we investigated the mechanism of protective effect of ASX on the onset of diabetic nephropathy, focusing on mesangial cells.

At first, we investigated whether or not HG might affect cellular viability of NHMCs, and found that HG did not affect cellular viability of

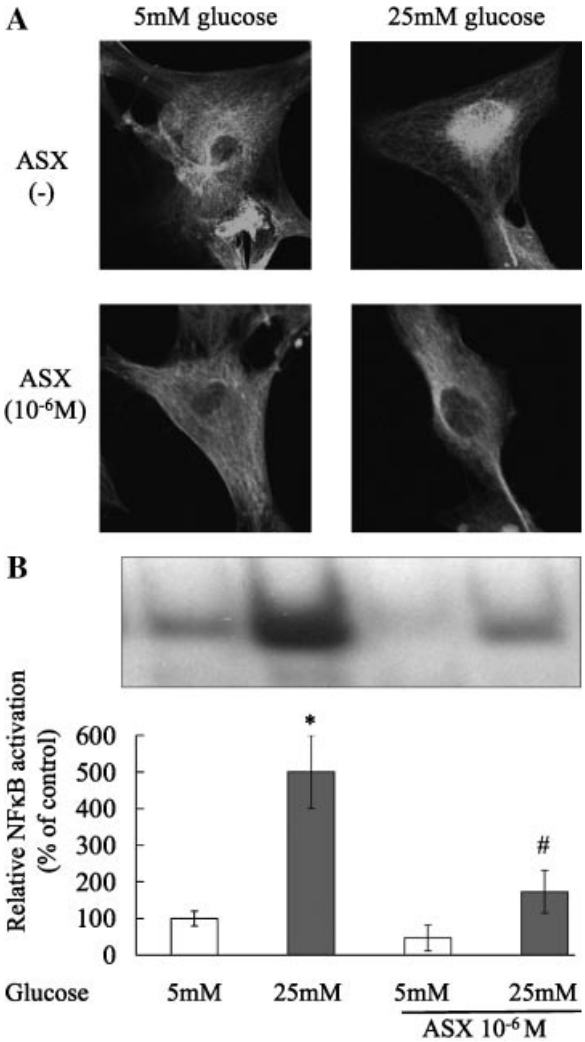

Fig. 3. ASX suppressed HG-induced nuclear translocation and activation of NFκB. **A**: Immunocytochemical images of NFκB nuclear translocation under the laser scanning confocal microscopy were shown. NHMCs treated with NG (**upper left**), HG (**upper right**), NG + ASX (**lower left**), and HG + ASX (**lower right**) were presented. In each panel, the image of FITC-conjugated NFκB (green fluorescence) localization was presented. Representative image out of three independent experiments was performed in triplicate samples. **B**: DNA-binding activity of NFκB was assessed by EMSA. Representative image out of three independent experiments was presented in **upper panel**. The result of densidometrical analysis shown in the **lower panel** is given as percentage variation of O.D. versus NG group. $^{*}P < 0.01$ versus NG group, $^{\#}P < 0.01$ versus HG group.

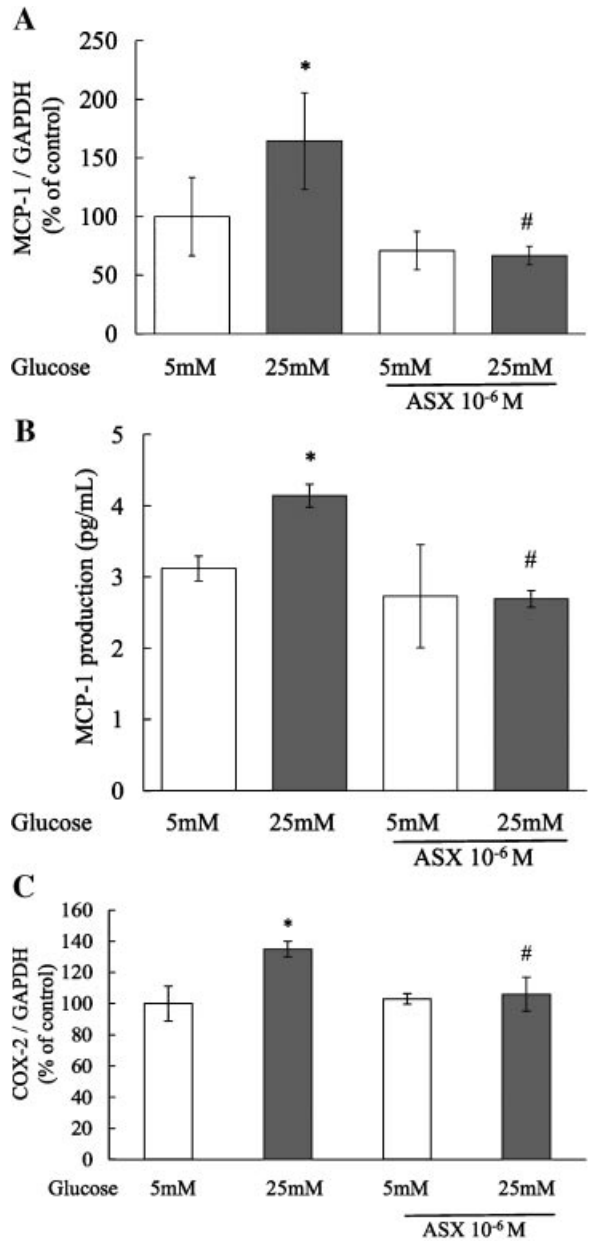

Fig. 4. ASX inhibited HG-induced MCP-1 expression/production and COX-2 expression by NHMCs. **A**: MCP-1 mRNA expression in NHMCs was assessed by RT-PCR. The relative MCP-1 mRNA expression was calculated as the density of the product of the respective target gene divided by that for GAPDH from the same cDNA. **B**: MCP-1 production in NHMCs culture supernatant was assessed by ELISA. **C**: COX-2 mRNA expression in NHMCs was assessed by RT-PCR. The relative COX-2 mRNA expression was calculated as the density of the product of the respective target gene divided by that for GAPDH from the same cDNA. Data are expressed as mean ± SEM of six independent experiments performed in triplicate in each assay. $^{*}P < 0.05$, $^{\#}P < 0.05$.

NHMCs within 48 h. HG (25 mM of D-glucose) is relevant to high serum glucose around 400 mg/dl in human body and NG (5 mM of D-glucose) is relevant to normal serum glucose around 90 mg/dl. On the contrary to our findings, it has been reported that HG induced proapoptotic signaling in NHMCs [Kang et al.,

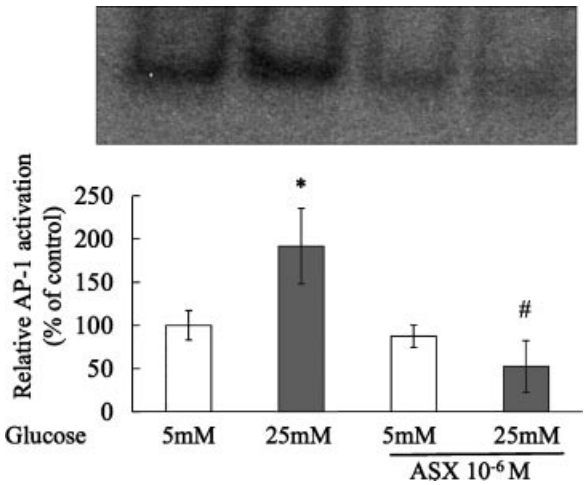

Fig. 5. ASX suppressed HG-induced AP-1 activation. Representative image out of three independent experiments was presented in **upper panel** as assessed by EMSA. The result of densidometrical analysis shown in the **lower panel** is given as percentage variation of O.D. versus NG group. $^{*}P < 0.01$ versus NG group, $^{\#}P < 0.01$ versus HG group.

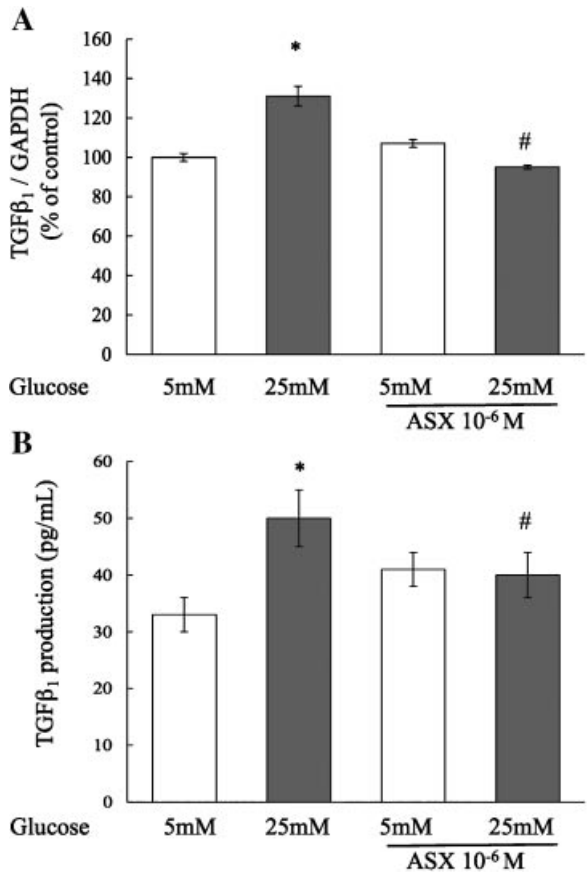

Fig. 6. ASX inhibited HG-induced $TGF\beta_1$ expression/production by NHMCs. **A**: $TGF\beta_1$ mRNA expression in NHMCs was assessed by RT-PCR. The relative $TGF\beta_1$ mRNA expression was calculated as the density of the product of the respective target gene divided by that for GAPDH from the same cDNA. **B**: TGF-β_1 production in NHMCs culture supernatant was assessed by ELISA. Data are expressed as mean ± SEM of six independent experiments performed in triplicate in each assay. $^{*}P < 0.05$, $^{\#}P < 0.05$.

2003; Mishra et al., 2005]. One of the reasons for this discrepancy between our and their study is that they [Mishra et al., 2005] cultured NHMCs in higher concentration of FBS (17%) and exposed NHMCs with higher concentration of D-glucose (30 mM) than that in our experiments (5% of FBS and 25 mM of D-glucose). Such high concentration of serum and glucose in the cell culture medium may cause excessive electron flow in the mitochondria of NHMCs and result in overproduction of cytotoxic ROS. Another possibility is that they [Kang et al., 2003; Mishra et al., 2005] used sub-confluent cell monolayers that are supposed to be more susceptible to glucose cytotoxicity than confluent cell monolayers might be. In addition, we could not detect apoptosis in HG-treated NHMCs by using Hoechest33342, a fluorescent probe that can detect apoptotic bodies in cells, a marker of apoptosis [Handa et al., 2006a] (data not shown).

Next, we found that HG induced ROS production in mitochondria of NHMCs. This is in consistent with the results obtained in previous reports in vitro [Kiritoshi et al., 2003] and in vivo [Naito et al., 2004, 2006]. With regard to the mechanism behind this, Lee et al. [2003] has reported that rotenone, an inhibitor of mitochondrial electron transport chain complex I, effectively blocked HG-induced ROS generation in mesangial cells, suggesting that ROS are produced in the transfer of electrons from complex I to ubiquinone in HG-treated NHMCs. In addition, Kiritoshi et al. [2003] reported that thenoyltrifluoroacetone (TTFA), an inhibitor of

TABLE I. ASX Content in Subcellular Fractions of NHMCs

	ASX content (% of added ASX)	
	Mitochondria	Cytosol
ASX 10^{-6} M	0.33 ± 0.12	0
ASX 10^{-5} M	0.16 ± 0.05	0

Values are means of three samples. Obtained quantity of ASX in total mitochondria of NHMCs (2.5×10^7 cells) in three samples were adjusted by added total ASX quantity, and expressed as % of added total ASX. There were no statistically significant differences between 10^{-6} M of ASX group and 10^{-5} M of ASX group.

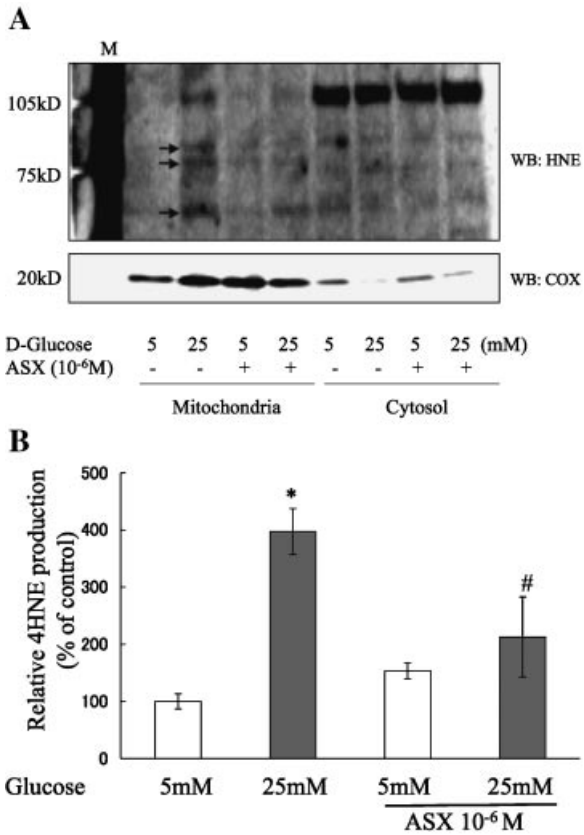

Fig. 7. ASX inhibited HG-induced production of oxidative stress-modified proteins in mitochondria of NHMCs. **A**: Representative Western blotting image out of three independent experiments was shown. Anti-4HNE antibody was used to detect protein adducts in mitochondrial- and cytosolic-fractions of HG-treated NHMCs. Anti-COX antibody was used as a mitochondrial protein marker. Arrows indicate bands stained with anti-4HNE antibody. M: marker. **B**: The result of densidometrical analysis of 4HNE in mitochondrial fraction is adjusted by that of COX and given as percentage variation of O.D. versus NG group. $^{*}P < 0.01$ versus NG group, $^{\#}P < 0.05$ versus HG group.

mitochondrial electron transport chain complex II, and carbonyl cyanide m-chlorophenylhydrazone (CCCP), an uncoupler of mitochondrial oxidative phosphorylation, as well as overexpression of uncoupling protein-1 (UCP-1) or manganese superoxide dismutase (MnSOD), an antioxidant enzyme, effectively blocked HG-induced ROS production in NHMCs, suggesting that the active involvement of mitochondrial electron transport system and intracellular enzymes in HG-induced ROS production in NHMCs. Although the mechanisms by which HG induces the dysfunction of mitochondrial transport system in mesangial cell is still unclear, the probable mechanism is that HG induces the production of advanced glycation end products (AGE) [Tuttle et al., 2005] that can produce ROS via the binding of AGE to its receptor (RAGE) on mesangial cells [Fukami et al., 2004]. However this issue should be further elucidated.

This HG-induced ROS production in NHMCs was effectively inhibited by ASX. In order to investigate the mechanism behind this phenomenon more in detail, we measured ASX concentrations in mitochondria and cytoplasm of NHMCs by HPLC, and found that ASX added to NHMCs primarily accumulated in the mitochondria fraction of NHMCs. Although the mechanism by which ASX inhibits the production of ROS must be further elucidated, we speculate that ASX might affect the mitochondria electron transport system, and protect mitochondria from the detrimental effects of HG, thereby inhibiting the production of ROS from mitochondria. In the present study, we showed the accumulation of ASX within mitochondria of NHMCs. To our knowledge, this is the first report that ASX accumulates in mitochondria of NHMCs and inhibits HG-induced ROS production in NHMCs. However it has been reported that ASX, liposoluble, could be detected within the cell membrane, same as α-carotene, β-carotene, and lycopene [Cantrell et al., 2003], and orally administrated ASX could accumulate in microsomes or sarcoplasmic reticulum as well as in mitochondria [Takahashi et al., 2004]. The discrepancy between these studies and ours might be mainly due to the time point of each study when ASX content was measured. Therefore in order to further identify the localization of ASX in organelle of NHMCs and to investigate the role of ASX on ROS production, the kinetic experiments should be needed in the future.

To further confirm the production of ROS in mitochondria of NHMCs, we assessed the production of 4HNE, a maker of oxidative lipid oxidation [Uchida, 2005], in mitochondria- and cytosolic-fractions in NHMCs. Our Western blotting analysis clearly showed that at least four bands having molecular size of about 60, 80, 85, and 105 kDa were strongly stained by anti-4HNE antibody in mitochondrial fraction of HG-treated NHMCs, suggesting the occurrence of lipid peroxidation mainly in mitochondria of HG-treated NHMCs. Moreover, these bands were less stained by anti-4HNE antibody in mitochondrial fraction of NG-treated, ASX-treated, or HG- and ASX-treated groups as well

as in cytosolic-fractions of all groups. These findings further confirmed that HG induced ROS production mainly via mitochondria-dependent pathway in NHMCs and that ASX specifically reduced HG-induced ROS production in the mitochondria of NHMCs. 4HNE protein adducts production were also found in cytosolic fraction, in lesser extent than that in mitochondria fraction, in HG-treated NHMCs that was suppressed by ASX pre-treatment. Since ROS and 4HNE-modified proteins produced in mitochondria have been reported to reduce mitochondrial function, resulting in more ROS production in mitochondria [Choksi et al., 2004], it is possible that excessive ROS production leaked from mitochondria could result in the production of HNE-modified proteins in cytosol and the suppression of ROS and 4HNE production in mitochondria by ASX might also reduce the ROS and 4HNE production in cytosol.

HG-induced ROS production changes redox status of mesangial cells resulting in the activation of the redox-sensitive transcription factors, NFκB and AP-1, which has been shown to play a key role in diabetic nephropathy [Guijarro and Egido, 2001; Mezzano et al., 2004]. For example, HG-induced NFκB activation resulted in the induction of COX-2 mRNA and protein, as well as PGE_2 synthesis in mesangial cells resulting in the glomerular hyperfiltration observed in the early stage of diabetes [Diaz-Cazorla et al., 1999; Kiritoshi et al., 2003]. Furthermore, the activation of NFκB resulted in the increased expression/production of MCP-1 mRNA and protein in mesangial cells that plays an important role in the inflammatory process and subsequent injury of mesangial area [Ha et al., 2002]. Similarly HG-induced ROS-dependent AP-1 activation has reported to increase $TGF\beta_1$ production in mesangial cells that plays a central role in the glomerular matrix production and pathogenesis of diabetic nephropathy [Lee et al., 2003]. Consistent with the previously reported findings, we found that HG exposure increased NFκB and AP-1 activation and subsequent expression/production of COX-2, MCP-1, and $TGF\beta_1$ in NHMCs. In addition, ASX effectively inhibited these events.

In the present study, we showed that HG induced the production of ROS-modified proteins (4HNE protein adducts) in the mitochondria of HG-treated NHMCs. We speculate that these ROS-modified proteins may contribute to the progression of diabetic nephropathy via COX-2, MCP-1, and $TGF\beta_1$ production by NHMCs, since many reports has shown that 4HNE induced COX-2 [Uchida and Kumagai, 2003], MCP-1 [Nitti et al., 2002], and $TGF\beta_1$ [Leonarduzzi et al., 1997] production. In these reports they showed that 4HNE stabilized COX-2 mRNA and induced its expression via p38 mitogen-activated protein kinase pathway, 4HNE induced MCP-1 production by increased activity of beta-PKC isoforms, and 4HNE induced both mRNA expression and synthesis of $TGF\beta_1$. To identify these ROS-modified proteins and their precise functions is very important and is now a matter of active investigation by using proteomics technology [Naito et al., 2007]. Although there are many reports that identified 4HNE-modified proteins in the cell, only a few reports identified 4HNE-modified proteins in mitochondria so far [Choksi et al., 2004]. In that report, Choksi et al. identified several proteins of 4HNE-modified mitochondrial respiratory chain complexes. However, the molecular weight of these proteins are smaller than that obtained in our study. The identification of these ROS-modified proteins in mitochondria is under investigation in our laboratory.

In summary, ASX added to NHMCs accumulated in the mitochondria, possibly scavenged overproduced ROS, reduced ROS-modified protein production and inhibited subsequent transcription factors activation and COX-2, MCP-1, and $TGF\beta_1$ production, thus might prevent the progression of diabetic nephropathy. ASX might be a novel and safety approach for the prevention of diabetic nephropathy.

REFERENCES

Baynes JW, Thorpe SR. 1999. Role of oxidative stress in diabetic complications: A new perspective on an old paradigm. Diabetes 48:1–9.

Bennedsen M, Wang X, Willen R, Wadstrom T, Andersen LP. 1999. Treatment of H. pylori infected mice with antioxidant astaxanthin reduces gastric inflammation, bacterial load and modulates cytokine release by splenocytes. Immunol Lett 70:185–189.

Cantrell A, McGarvey DJ, Truscott TG, Rancan F, Bohm F. 2003. Singlet oxygen quenching by dietary carotenoids in a model membrane environment. Arch Biochem Biophys 412:47–54.

Catherwood MA, Powell LA, Anderson P, McMaster D, Sharpe PC, Trimble ER. 2002. Glucose-induced oxidative stress in mesangial cells. Kidney Int 61:599–608.

Cepinskas G, Savickiene J, Ionescu CV, Kvietys PR. 2003. PMN transendothelial migration decreases nuclear

NFkappaB in IL-1beta-activated endothelial cells: Role of PECAM-1. J Cell Biol 161:641–651.
Chew BP, Park JS, Wong MW, Wong TS. 1999. A comparison of the anticancer activities of dietary beta-carotene, canthaxanthin and astaxanthin in mice in vivo. Anticancer Res 19:1849–1853.
Choksi KB, Boylston WH, Rabek JP, Widger WR, Papaconstantinou J. 2004. Oxidatively damaged proteins of heart mitochondrial electron transport complexes. Biochim Biophys Acta 1688:95–101.
Coral-Hinostroza GN, Ytrestoyl T, Ruyter B, Bjerkeng B. 2004. Plasma appearance of unesterified astaxanthin geometrical E/Z and optical R/S isomers in men given single doses of a mixture of optical 3 and 3'R/S isomers of astaxanthin fatty acyl diesters. Comp Biochem Physiol C Toxicol Pharmacol 139:99–110.
Coughlan MT, Cooper ME, Forbes JM. 2007. Renal microvascular injury in diabetes: RAGE and redox signaling. Antioxid Redox Signal 9:331–342.
Diaz-Cazorla M, Perez-Sala D, Lamas S. 1999. Dual effect of nitric oxide donors on cyclooxygenase-2 expression in human mesangial cells. J Am Soc Nephrol 10:943–952.
Fukami K, Ueda S, Yamagishi S, Kato S, Inagaki Y, Takeuchi M, Motomiya Y, Bucala R, Iida S, Tamaki K, Imaizumi T, Cooper ME, Okuda S. 2004. AGEs activate mesangial TGF-beta-Smad signaling via an angiotensin II type I receptor interaction. Kidney Int 66:2137–2147.
Fukuzawa K, Inokami Y, Tokumura A, Terao J, Suzuki A. 1998. Rate constants for quenching singlet oxygen and activities for inhibiting lipid peroxidation of carotenoids and alpha-tocopherol in liposomes. Lipids 33:751–756.
Guijarro C, Egido J. 2001. Transcription factor-kappa B (NF-kappa B) and renal disease. Kidney Int 59:415–424.
Ha H, Lee HB. 2001. Oxidative stress in diabetic nephropathy: Basic and clinical information. Curr Diab Rep 1:282–287.
Ha H, Yu MR, Choi YJ, Kitamura M, Lee HB. 2002. Role of high glucose-induced nuclear factor-kappaB activation in monocyte chemoattractant protein-1 expression by mesangial cells. J Am Soc Nephrol 13:894–902.
Handa O, Naito Y, Takagi T, Shimozawa M, Kokura S, Yoshida N, Matsui H, Cepinskas G, Kvietys PR, Yoshikawa T. 2004. Tumor necrosis factor-alpha-induced cytokine-induced neutrophil chemoattractant-1 (CINC-1) production by rat gastric epithelial cells: Role of reactive oxygen species and nuclear factor-kappaB. J Pharmacol Exp Ther 309:670–676.
Handa O, Kokura S, Adachi S, Takagi T, Naito Y, Tanigawa T, Yoshida N, Yoshikawa T. 2006a. Methylparaben potentiates UV-induced damage of skin keratinocytes. Toxicology 227:62–72.
Handa O, Yoshida N, Fujita N, Tanaka Y, Ueda M, Takagi T, Kokura S, Naito Y, Okanoue T, Yoshikawa T. 2006b. Molecular mechanisms involved in anti-inflammatory effects of proton pump inhibitors. Inflamm Res 55:476–480.
Hinokio Y, Suzuki S, Hirai M, Chiba M, Hirai A, Toyota T. 1999. Oxidative DNA damage in diabetes mellitus: Its association with diabetic complications. Diabetologia 42:995–998.
Inoguchi T, Li P, Umeda F, Yu HY, Kakimoto M, Imamura M, Aoki T, Etoh T, Hashimoto T, Naruse M, Sano H, Utsumi H, Nawata H. 2000. High glucose level and free fatty acid stimulate reactive oxygen species production through protein kinase C-dependent activation of NAD(P)H oxidase in cultured vascular cells. Diabetes 49:1939–1945.
Jyonouchi H, Zhang L, Gross M, Tomita Y. 1994. Immunomodulating actions of carotenoids: Enhancement of in vivo and in vitro antibody production to T-dependent antigens. Nutr Cancer 21:47–58.
Jyonouchi H, Sun S, Tomita Y, Gross MD. 1995. Astaxanthin, a carotenoid without vitamin A activity, augments antibody responses in cultures including T-helper cell clones and suboptimal doses of antigen. J Nutr 125: 2483–2492.
Kaneto H, Katakami N, Kawamori D, Miyatsuka T, Sakamoto K, Matsuoka TA, Matsuhisa M, Yamasaki Y. 2007. Involvement of oxidative stress in the pathogenesis of diabetes. Antioxid Redox Signal 9:355–366.
Kang BP, Frencher S, Reddy V, Kessler A, Malhotra A, Meggs LG. 2003. High glucose promotes mesangial cell apoptosis by oxidant-dependent mechanism. Am J Physiol Renal Physiol 284:F455–F466.
Kiritoshi S, Nishikawa T, Sonoda K, Kukidome D, Senokuchi T, Matsuo T, Matsumura T, Tokunaga H, Brownlee M, Araki E. 2003. Reactive oxygen species from mitochondria induce cyclooxygenase-2 gene expression in human mesangial cells: potential role in diabetic nephropathy. Diabetes 52:2570–2577.
Kobayashi M. 2000. In vivo antioxidant role of astaxanthin under oxidative stress in the green alga Haematococcus pluvialis. Appl Microbiol Biotechnol 54:550–555.
Kurihara H, Koda H, Asami S, Kiso Y, Tanaka T. 2002. Contribution of the antioxidative property of astaxanthin to its protective effect on the promotion of cancer metastasis in mice treated with restraint stress. Life Sci 70:2509–2520.
Lee HB, Yu MR, Yang Y, Jiang Z, Ha H. 2003. Reactive oxygen species-regulated signaling pathways in diabetic nephropathy. J Am Soc Nephrol 14:S241–S245.
Leonarduzzi G, Scavazza A, Biasi F, Chiarpotto E, Camandola S, Vogel S, Dargel R, Poli G. 1997. The lipid peroxidation end product 4-hydroxy-2,3-nonenal up-regulates transforming growth factor beta1 expression in the macrophage lineage: a link between oxidative injury and fibrosclerosis. Faseb J 11:851–857.
Lok CE, Oliver MJ, Rothwell DM, Hux JE. 2004. The growing volume of diabetes-related dialysis: A population based study. Nephrol Dial Transplant 19:3098–3103.
Mezzano S, Aros C, Droguett A, Burgos ME, Ardiles L, Flores C, Schneider H, Ruiz-Ortega M, Egido J. 2004. NF-kappaB activation and overexpression of regulated genes in human diabetic nephropathy. Nephrol Dial Transplant 19:2505–2512.
Mishra R, Emancipator SN, Kern T, Simonson MS. 2005. High glucose evokes an intrinsic proapoptotic signaling pathway in mesangial cells. Kidney Int 67:82–93.
Naguib YM. 2000. Antioxidant activities of astaxanthin and related carotenoids. J Agric Food Chem 48:1150–1154.
Naito Y, Uchiyama K, Aoi W, Hasegawa G, Nakamura N, Yoshida N, Maoka T, Takahashi J, Yoshikawa T. 2004. Prevention of diabetic nephropathy by treatment with astaxanthin in diabetic db/db mice. Biofactors 20:49–59.
Naito Y, Uchiyama K, Mizushima K, Kuroda M, Akagiri S, Takagi T, Handa O, Kokura S, Yoshida N, Ichikawa H, Takahashi J, Yoshikawa T. 2006. Microarray profiling of

gene expression patterns in glomerular cells of astaxanthin-treated diabetic mice: A nutrigenomic approach. Int J Mol Med 18:685–695.

Naito Y, Takagi T, Yoshikawa T. 2007. Neutrophil-dependent oxidative stress in ulcerative colitis. J Clin Biochem Nutr 41:18–26.

Nakai S, Wada A, Kitaoka T, Shinzato T, Nagura Y, Kikuchi K, Masakane I, Shinoda T, Yamazaki C, Sakai R, Marubayashi S, Morita O, Iseki K, Usami T, Kimata N, Suzuki K, Tabei K, Fushimi K, Miwa N, Yauchi M, Wakai K, Akiba T. 2006. An overview of regular dialysis treatment in Japan (as of 31 December 2004). Ther Apher Dial 10:476–497.

Nishikawa T, Edelstein D, Du XL, Yamagishi S, Matsumura T, Kaneda Y, Yorek MA, Beebe D, Oates PJ, Hammes HP, Giardino I, Brownlee M. 2000. Normalizing mitochondrial superoxide production blocks three pathways of hyperglycaemic damage. Nature 404:787–790.

Nishikawa T, Kukidome D, Sonoda K, Fujisawa K, Matsuhisa T, Motoshima H, Matsumura T, Araki E. 2007. Impact of mitochondrial ROS production on diabetic vascular complications. Diabetes Res Clin Pract 77:S41–S45.

Nitti M, Domenicotti C, d'Abramo C, Assereto S, Cottalasso D, Melloni E, Poli G, Biasi F, Marinari UM, Pronzato MA. 2002. Activation of PKC-beta isoforms mediates HNE-induced MCP-1 release by macrophages. Biochem Biophys Res Commun 294:547–552.

Ohgami K, Shiratori K, Kotake S, Nishida T, Mizuki N, Yazawa K, Ohno S. 2003. Effects of astaxanthin on lipopolysaccharide-induced inflammation in vitro and in vivo. Invest Ophthalmol Vis Sci 44:2694–2701.

Suzuki S, Hinokio Y, Komatu K, Ohtomo M, Onoda M, Hirai S, Hirai M, Hirai A, Chiba M, Kasuga S, Akai H, Toyota T. 1999. Oxidative damage to mitochondrial DNA and its relationship to diabetic complications. Diabetes Res Clin Pract 45:161–168.

Takahashi K, Watanabe M, Takimoto T, Akiba Y. 2004. Uptake and distribution of astaxanthin in several tissues and plasma lipoproteins in male broiler chickens fed a yeast (Phaffia rhodozyma) with a high concentration of astaxanthin. Br Poult Sci 45:133–138.

Tuttle KR, Johnson EC, Cooney SK, Anderberg RJ, Johnson EK, Clifton GD, Meek RL. 2005. Amino acids injure mesangial cells by advanced glycation end products, oxidative stress, and protein kinase C. Kidney Int 67:953–968.

Uchida K. 2005. Protein-bound 4-hydroxy-2-nonenal as a marker of oxidative stress. J Clin Biochem Nutr 36: pp 1–10.

Uchida K, Kumagai T. 2003. 4-hydroxy-2-nonenal as a COX-2 inducer. Mol Aspects Med 24:213–218.

Uchiyama K, Naito Y, Hasegawa G, Nakamura N, Takahashi J, Yoshikawa T. 2002. Astaxanthin protects beta-cells against glucose toxicity in diabetic db/db mice. Redox Rep 7:290–293.

Wild S, Roglic G, Green A, Sicree R, King H. 2004. Global prevalence of diabetes: Estimates for the year 2000 and projections for 2030. Diabetes Care 27:1047–1053.

Ziyadeh FN. 1993. The extracellular matrix in diabetic nephropathy. Am J Kidney Dis 22:736–744.